Pedagogical Supplement

S. R. Kulkarni

May 30, 2019–November 29, 2019

1 Background & Motivation

This is a "pedagogical supplement" to the paper "Contrails in the radio sky" by S. R. Kulkarni (in prep.).[1] The paper is concerned about the physical evolution of dense gas ($n_e \sim 10^2$ to $10^3\,\mathrm{cm}^{-3}$) which is invoked to explain extreme scattering events and related phenomenon. The paper does not rely on this supplement. The supplement is useful for graduate students who are not familiar with the topics discussed in the paper. The notes are organized as follows. In (§2) and (§3) I summarize the essential physics involved in cooling and ionization and heating, respectively. In §4, using the results in §2 and §3 I reproduce the classic equilibrium temperature and ionization of the two phases of the atomic interstellar medium (ISM): the Cold Neutral Medium and the Warm Neutral Medium. In §5, I apply my newly developed numerical suite to a novel situation: a nebula which is irradiated by strong flux of cosmic rays.

[1]The paper arose of out my visit to the Netherlands as a van der Waals Visiting Professor at the University of Amsterdam, NL. It was expected that I would give three lectures. My first lecture was a colloquium on my current research (the Zwicky Transient Facility). The students and postdocs were intrigued with my research style, namely switching topics every now and then. This led me to giving my second lecture on on "How (and why) to change research areas?". I then decided that the best way to demonstrate a concept is a live demonstration. To this end, I chose a new project and worked on that feverishly and the preliminary findings – the paper discussed above – constituted my third lecture.

I attended a LOFAR annual symposium at Leiden and listened carefully to the talks. It became clear to me that while there has been great progress in low frequency astronomy (LOFAR, MWA, LWA) particularly in amassing of data there was less progress, relatively speaking, in our physical understanding. This opened an opportunity for an old fox like me to reenter the field!

Following the Leiden LOFAR meeting I decided to visit the topic of extreme-scattering events and related phenomena. I was broadly familiar with the basic concepts and physics germane for the proposed investigation. However, I did not have the necessary precision understanding to undertake numerical modeling. To this end I undertook a self-taught course making "deep dives" into three textbooks: Draine (2011), Tielens (2005) and the classic book by Spitzer (1978). I reproduced critical figures in the relevant chapters of these books and satisfied myself that my understanding was precise. Along the way I wrote notes to myself so that I could use the notes for teaching a graduate level course.

2 Cooling

The principal cooling lines are fine structure lines of C II and O I and recombination of electrons and atoms on dust. In steady state, free-bound and free-free radiation of electrons are minor contributors. Only when the temperature approaches 10^4 K does cooling from Lyman alpha and forbidden line of OI become important.

2.1 Fine structure line of C II

The ground configuration of C II (or C^+, for short) is $1s^2 2s^2 2p^1$ consists of the ground level (subscript, "l") $^2P_{1/2}$ ($g_0 = 2$) and the upper level ("u") $^2P_{3/2}$ ($g_1 = 4$) separated by $E_{10}/k_B = 91.21$ K. The radiative de-excitation of the upper level results in the famous 157.7 μm line. The A_{10}, the A-coefficient for this $1 \rightarrow 0$ transition is $2.4 \times 10^{-6}\,\mathrm{s}^{-1}$.

It is traditional to quote de-excitation coefficients, k_{ul} where u refers to the upper level and l to the lower level. For all electron-ion interactions it is conventional to state k_{ul} in the following form:

$$k_{ul}(e) = \frac{8.629 \times 10^{-8}}{\sqrt{T_4}} \frac{\Omega_{ul}}{g_u}\,\mathrm{cm}^3\,\mathrm{s}^{-1} \tag{1}$$

where Ω_{ul} is the "collisional strength" and the $T^{-1/2}$ factor accounts for Coulomb focusing. From the principle of detailed balance we know that the de-excitation coefficient is related to the excitation coefficient (k_{lu}) as follows

$$\frac{k_{lu}(T)}{k_{ul}(T)} = \frac{g_u}{g_l} \exp\Big(-\frac{E_{ul}}{k_B T}\Big) \equiv R. \tag{2}$$

For the C^+ line the experimental data are modeled as

$$\Omega_{10} = \frac{1.55 + 1.25 T_4}{1 + 0.35 T_4^{1.25}} \tag{3}$$

(Draine 2011; [D11]; Table F.1). Over the range 10–10^3 K, Ω_{10} ranges from 1.55 to 1.65. Following Draine (2011; [D11]) we adopt a mean value of 1.6. Thus,

$$k_{10}(e^-) \approx 3.45 \times 10^{-8} T_4^{-1/2}\,\mathrm{cm}^{-3}\,\mathrm{s}^{-1}. \tag{4}$$

The de-excitation coefficient for H I is

$$k_{10}(\mathrm{H}) \approx 7.58 \times 10^{-10} T_2^{0.1281 + 0.0087 \ln(T_2)}\,\mathrm{cm}^{-3}\,\mathrm{s}^{-1} \tag{5}$$

and that for helium is $k_{10}(\mathrm{He}) = 0.38 k_{10}(\mathrm{H})$ (Draine 2011; [D11]; Table F.6). Since, by number, helium is 10% of hydrogen, the former increases H excitation by only 3.8%. `He collisions are not included in my MATLAB routine-- yet`.

Considering only collisions by electrons, in equilibrium, the rate of excitation per unit volume is $n_e n_0 k_{01}$ is balanced by $n_1(n_e k_{10} + A_{10})$. Here, n_0 and n_1 is the number density of C^+ ions in the ground state and excited state, respectively. After some manipulation it can be shown that

$$\frac{n_1}{n_t} = \frac{R}{1 + n_{\rm cr}/n_e + R} \tag{6}$$

where $n_t = n_0 + n_1$ and the "critical density", $n_{\rm cr} \equiv A_{10}/k_{10}$. The radiative loss per unit time per unit volume is

$$\mathcal{L} = n_1 A_{10} E_{10} = n_t A_{10} E_{10} \frac{R}{1 + R + n_{\rm cr}/n_e}. \tag{7}$$

For $n_e \ll n_{\rm cr}$, we expect every collision to result in emission of a photon and indeed find that $\mathcal{L} \approx n_t n_e k_{01} E_{10}$. For $n_e \gg n_{\rm cr}$, the levels are populated by the Boltzmann distribution and radiative losses saturates (that is, $\mathcal{L}$ no scales linearly with n_e) to $n_t A_{10} E_{10} R/(1+R)$. The critical density for electron collisions varies from $3\,{\rm cm}^{-3}$ (at $T = 30\,{\rm K}$) to $47\,{\rm cm}^{-3}$ (at $T = 8000\,{\rm K}$). In contrast, the critical density for collisions with H atoms varies from $3600\,{\rm cm}^{-3}$ to $1500\,{\rm cm}^{-3}$ over the same range of temperature.

Moving on, Equation 6 can be generalized to include excitation by electrons and H atoms:

$$\frac{n_1}{n_t} = \frac{R}{1 + R + A_{10}/C} \tag{8}$$

where $C = n_e k_{10}(e) + n_{\rm H} k_{10}({\rm H})$. The radiative loss per unit time per unit volume is then

$$\mathcal{L}({\rm C}^+) = n_b A_C A_{10} E_{10} \frac{R}{1 + R + A_{10}/C}\ {\rm erg\,cm^{-3}\,s^{-1}}, \tag{9}$$

where A_C is the abundance of carbon in gas phase, by number, to that of hydrogen. We adopt $A_C = 1 \times 10^{-4}$. The usual "cooling function" is $\Lambda \equiv \mathcal{L}/n_b^2$.

2.2 Fine-structure lines of O I

The ground configuration of O I is $1s^2 2s^2 2p^4$ which splits into three fine structure levels: $^3{\rm P}_2$ (ground), $^3{\rm P}_1$ (level 1) and $^3{\rm P}_0$ (level 2). The temperature equivalent of the 1 and 2 energy states is $T_1 = 227\,{\rm K}$ and $T_2 = 326\,{\rm K}$. The famous OI $63.18\,\mu$m fine structure line is the transition from $1 \rightarrow 0$ ($A_{10} = 8.95 \times 10^{-5}\,{\rm s}^{-1}$). The lesser known $145.53\,\mu$m line ($A_{21} = 1.7 \times 10^{-5}\,{\rm s}^{-1}$) results from $2 \rightarrow 1$ de-excitations. The $2 \rightarrow 0$ transition is forbidden,[2] $A_{20} = 1.34 \times 10^{-10}\,{\rm s}^{-1}$. The OI fine structure lines play an important role in the cooling of WNM (Draine 2011; [D11]; §17.6).

[2] A-coefficient obtained from the Leiden and Atomic Molecular Database (LAMDA): `https://home.strw.leidenuniv.nl/~moldata/`

The OI-H collisional coefficients are from from Draine (2011; [D11]; Appendix F):

$$k_{10}(H) = 3.57\times10^{-10}T_2^{0.419-0.003\ln T_2}\,\mathrm{cm^3\,s^{-1}} \quad (10)$$
$$k_{20}(H) = 3.19\times10^{-10}T_2^{0.369-0.006\ln T_2}\,\mathrm{cm^3\,s^{-1}} \quad (11)$$
$$k_{21}(H) = 4.34\times10^{-10}T_2^{0.755-0.160\ln T_2}\,\mathrm{cm^3\,s^{-1}}. \quad (12)$$

For the electron de-excitation we use the revised coefficients given in the Errata of Draine 2011 ([D11]; first edition)[3] where the collisional strengths are given by

$$\Omega_{10}(e) = 0.0105T_4^{0.4861+0.0054\ln(T_4)} \quad (13)$$
$$\Omega_{20}(e) = 0.00459T_4^{0.4507-0.0066\ln(T_4)} \quad (14)$$
$$\Omega_{21}(e) = 0.00015T_4^{0.4709-0.1396\ln(T_4)}. \quad (15)$$

We verified that the resulting de-excitation coefficients are in line with those at the LAMDA website. The electron de-excitation coefficient is very weakly dependent on temperature (in line with the fact that this is an electron-neutral collision) whereas the H de-excitation coefficient increases with increasing temperature.

There are two other colliders that should be considered: molecular hydrogen and protons (T05). We discount the former by stopping our calculation when molecules start forming (new excitation and radiation channels open up and considerations of these is beyond the ability of the author). The latter can be quite important since it is well known that ion-neutral reactions have large cross-sections (arising from the polarization of the neutral by the ion) that are essentially independent of temperature (see Draine 2011, D11; §2.4). From Tielens (2005; [T05]; Table 2.7)) we find $k_{10}(\mathrm{H^+}) \approx 1.4\times10^{-8}\,\mathrm{cm^3\,s^{-1}}$, $k_{20}(\mathrm{H^+}) \approx 1.4\times10^{-8}\,\mathrm{cm^3\,s^{-1}}$ and $k_{21}(\mathrm{H^+}) \approx 5\times10^{-9}\,\mathrm{cm^3\,s^{-1}}$ and we assume that these coefficients are independent of temperature. I remark here that for typical CNM or WNM parameters the principal excitation is via H collisions and so including proton excitation results in a few percent additional luminosity.

For a multi-level system the critical density is justifiably given by

$$n_{\rm cr} = \frac{A_{ul}}{\sum_{0\le l'\le l} k_{ul'}} \quad (16)$$

where the sum in the denominator is over all possible de-excitations to lower levels. For the $1\rightarrow0$ transition the critical electron density range is $2.5\times10^5\,\mathrm{cm^{-3}}$ to $2.9\times10^5\,\mathrm{cm^{-3}}$

[3]Specifically, see Table F.3, p498 on page 23 of the Errata. As an aside we note the fitting formula for the O I-electron interactions is given, curiously, in a form that is appropriate for ion-electron interaction even though this is an electron-neutral interaction. It should be simply interpreted as a fitting formula. but not motivated by physical considerations. Note that the de-excitation coefficient is almost independent of temperature.

and that for H atoms is $2.5 \times 10^5\,\mathrm{cm}^{-3}$ to $5.1 \times 10^4\,\mathrm{cm}^{-3}$. For the $2 \rightarrow 1$ transition, the electron critical density varies from $2.2 \times 10^4\,\mathrm{cm}^{-3}$ (at $T = 100\,\mathrm{K}$) to $5.8 \times 10^3\,\mathrm{cm}^{-3}$ (at $T \approx 5,000\,\mathrm{K}$). Over the same temperature range, that for H-atoms ranges from $2.3 \times 10^4\,\mathrm{cm}^{-3}$ to $8.7 \times 10^3\,\mathrm{cm}^{-3}$. The corresponding critical densities from collisions with protons are $9 \times 10^3\,\mathrm{cm}^{-3}$ $(1 \rightarrow 0)$ and $1.5 \times 10^3\,\mathrm{cm}^{-3}$ $(2 \rightarrow 1)$, respectively.

We use the full 3-level solution to derive ratio of the population of level 1 ($f_1 = n_1/n_0$) and level 2 ($f_2 = n_2/n_0$) with respect to level 0 (Draine (2011; [D11]; §17.5). The volumetric luminosity in the two lines is then

$$\mathcal{L}(\mathrm{OI}) = \frac{n_b A_O}{1 + f_1 + f_2}\Big(f_1 A_{10} E_{10} + f_2 A_{21} E_{21}\Big)\,\mathrm{erg\,cm^{-3}\,s^{-1}} \tag{17}$$

where $E_{10} = k_B T_1$, $E_{21} = k_B(T_2 - T_1)$ and $A_O = 5 \times 10^{-4}$ is the cosmic abundance of oxygen (and assumed to be largely in the gas phase) relative to that of hydrogen, by number.

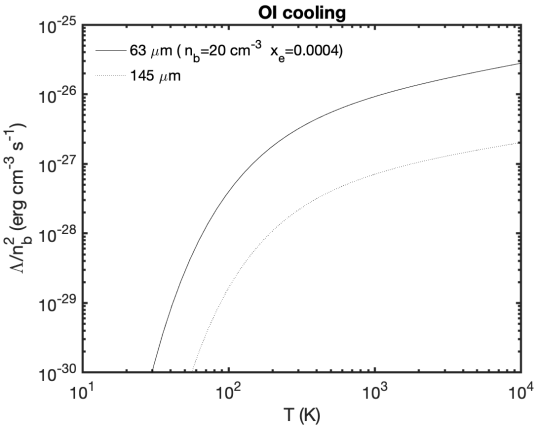

Figure 1: Cooling via the two fine fine structure lines of OI.

In Figure 1 I plot the cooling via the two OI fine structure lines for typical CNM. This figure should be compared with Figure 30.1 of Draine (2011; [D11]). In both the CNM and WNM there is not much cooling through the 145 μm line. So a simplified model can ignore the second excited state ($^3\mathrm{P}_0$). In effect, the OI fine structure system can be regarded as a two-level system ($^3\mathrm{P}_2$, ground state and $^3\mathrm{P}_1$, excited state) and the formulation stated in Equation 9 can be used with appropriate excitation coeffcients.

2.3 Cooling from H I Resonance Line Excitation

For warm gas, the primary loss channel is electronic excitation of H I atoms to the $n = 2$ state. This excitation dominates when temperature exceeds $10^4\,\mathrm{K}$. Spitzer (1978; [S78];

§6.2a) provides a fitting formula[4]

$$L_{e\mathrm{H}} = 7.3 \times 10^{-19} n_e n_H \exp(-118,400/T)\,\mathrm{erg\,cm^{-3}\,s^{-1}}, \tag{18}$$

which is valid for temperatures between 4,000 K and 12,000 K. Next, using $\langle \sigma v \rangle$ from Draine (2011; [D11]; Table 2.1) I find the volumetric luminosity from proton excitation (to the $n = 2$ state) is

$$L_{p\mathrm{H}} = 0.44 \times 10^{-19} n_p n_H \exp(-118,400/T)\,\mathrm{erg\,cm^{-3}\,s^{-1}}, \tag{19}$$

independent of temperature (see above). Clearly, excitation by protons provides a minor contribution, relative to that from electron excitation, to the cooling luminosity. For completeness I include collisional ionization of H I by electron impact:

$$L_{\mathrm{i,H}} = 1.27 \times 10^{-21} T^{1/2} n_e n_H \frac{\exp(-1.578 \times 10^5/T)}{1 + (T/1.58 \times 10^6)}\ \mathrm{erg\,cm^{-3}\,s^{-1}} \tag{20}$$

(Shull & Woods 1985; [sw85]). However, over the temperature range of interest, $T \lesssim 10^4$ K, the loss due to ionization is even smaller than the loss via resoance line cooling from proton excitation. The summary is that Equation 18 sufficiently captures the cooling losses in the temperature range of interest to this paper.

`What about ionization by protons? Is it smaller because of velocity difference?`

2.4 Cooling from recombination

An electron with velocity v recombines with a proton to level j of the H I atom and in the process radiates away energy equal to the sum of the kinetic energy, $1/2 m_e v^2$ and the electrostatic potential of the level. The electron rapidly then cascades down to deeper energy states radiating line photons along the way. Nonetheless, the energy lost from the thermal store is only the kinetic energy of the electron.The loss of energy per unit time per unit volume from free-bound process is

$$L_{\mathrm{fb}} = n_e^2 \sum_j \left\langle \frac{1}{2} m_e v^2 \sigma_{cj}(v) v \right\rangle \tag{21}$$

where the angular bracket implies averaging over the Maxwellian distribution of velocity and $\sigma_{cj}(v)$ is the cross-section for an electron with velocity v ("continuum") to be captured to level j and is $\propto g_{jf} j^{-3} (1/2 m_e v^2)^{-1}$ where g_{jf} is the "Gaunt" factor for level j (Spitzer 1978, [S78]; §5.1, §6.1). Clearly, recombination to deeper states is favored, as is the preference for slow moving electrons.

[4]See Table 2 of Dalgarno & McCray 1968 [dm72] for data.

We can re-express Equation 21 as $L_{\rm fb} = \alpha f_{\rm fb} k_B T$ where α is the recombination rate (case A or case B, as needed) which would then allow us to interpret $f_{\rm fb} k_B T$ as the average energy lost from the thermal bath per recombination. In Figure 2, we display the value of $f_{\rm fb}$ as a function of temperature. We find the following simple fits for $f_{\rm fb}$:

$$f_{\rm fb}({\rm caseA}) = 0.89 - 0.06 \log(T_2) \quad (22)$$

$$f_{\rm fb}({\rm caseB}) = 0.87 - 0.11 \log(T_2) \quad (23)$$

where $T_2 = T/10^2$. Thus, per recombination, the free-bound loss (case B) is $0.87 k_B T$ to $0.65 k_B T$.

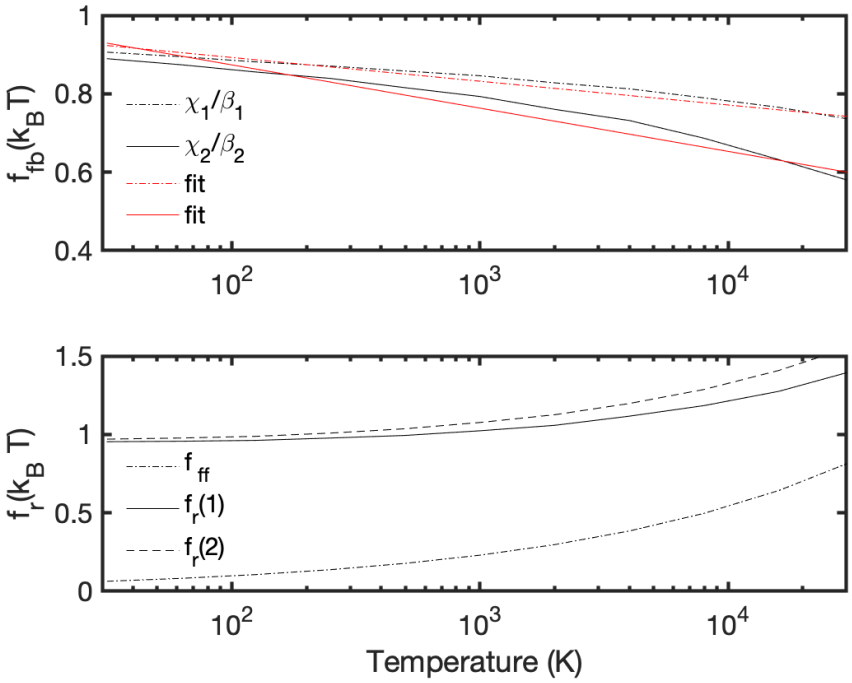

Figure 2: [Top] The mean energy of the recombining electron, $f_{\rm fb}$, for case A (subscript index 1) and case B (index 2). It can be shown that $L_{\rm fb}/\alpha = \chi/\beta$ where these two functions, over the range 30 K to 64,000 K, are tabulated in Tables 5.2 and 6.2 of Spitzer (1978; [S78]). The red lines show a simple linear fit to $f_{\rm fb}$. [Bottom]. Run of $f_{\rm ff}$ (Equation 24) as a function of temperature (black, dash-dot) and $f_r(j) \equiv f_{\rm ff} + f_{\rm fb}(j)$ (see Top) where $j = 1$ is recombination to level $n = 1$ and $j = 2$ is recombination to level $n = 2$.

Following Draine (2011; [D11];§27.32.) we consider the ratio of the volumetric rate of free-free cooling to the recombination rate and find

$$f_{\rm ff} \equiv \frac{L_{\rm ff}}{n_e^2 \alpha_B} = 0.54 T_4^{0.37} k_B T. \quad (24)$$

However, note that this approximation is *valid for WIM-like temperatures* (`read Rybiki and derive a fitting formula at lower temperatures`). Ignoring this caveat, the loss per recombination varies from $0.18 k_B T$ (cold gas) to $0.54 k_B T$ (warm gas). Thus, over the entire temperature range of interest, the cooling from free-bound (Equation 23) and free-free (Equation 24) add to yield, rather conveniently $f_r = f_{\rm ff} + f_{\rm fb} \approx 1 k_B T$ loss per recombination (case B).

In §3.2 we will discuss the cooling due to recombination of electrons and atoms onto grains.

3 Ionization & Heating

In the previous section we discussed cooling. Here, we discuss heating of the ISM. There are three microscopic heating processes which also result in providing electrons: photoelectric ionization & heating of C^0 (§3.1), photoelectric ionization & heating by dust particles including Polycyclic Aromatic Hydrocarbons (PAH; §3.2) and ionization & heating by cosmic rays (§3.3).

3.1 Photoelectric Ionization of & Heating by C^0

The far-UV (FUV) stellar radiation field can ionize metals provided their ionization potential is below that of H I. Of the FUV-photoionizable metals C, Na, Mg, Si, S, Fe, Al and Ca it is carbon that provides two thirds of the electrons (Draine 2011; [D11]; Table 9.5). So we will focus on ionization of carbon. The ionization potential of carbon is 11.3 eV. Thus the FUV field of interest is in the range 11.3–13.6 eV.

The stellar radiation field is usually stated in terms of a relative factor, G_0, where the base is the stellar radiation density originally determined by H. Habing (Tielens 2005; T05; Table 8.1). The average energy of the photoelectrons, $\langle E_{\rm C^0} \rangle$, appears to $\approx$ 1 eV (after accounting for the rapid decrease of FUV stellar radiation field as it approaches 912 Å; see Tielens 2005; T05; §3.2). The FUV photo-ionization rate per C I atom is

$$\zeta({\rm C^0}) = 2.58 \times 10^{-10} G_0 \exp(-2.6 {\rm A_V}) \ {\rm s^{-1}} \tag{25}$$

where the V-band extinction, A_V, accounts for extinction within the cloud (Draine 2011;[D11]; Table 13.1). `Check with Wolfire if 1 eV per ionization is the standard practice.`

It is instructive to carry out a pedagogical exercise in which carbon acts as the sole heating, ionizing and cooling source. In steady state, the rate of ionization per unit volume is matched by the rate of recombinations in the same volume:

$$\zeta({\rm C^0})[1 - x({\rm C^+})] = n_e x({\rm C^+}) \alpha_{rr}({\rm C^+}) \tag{26}$$

where $x(\mathrm{C}^+)$ is the fraction of C^+ relative to the total number of carbon nuclei. The ionized carbon fraction is then

$$x(\mathrm{C}^+) = \frac{\zeta(\mathrm{C}^0)}{\zeta(\mathrm{C}^0) + n_e \alpha_{rr}(\mathrm{C}^+)}. \tag{27}$$

The radiative recombination coefficient for carbon is

$$\alpha_{rr}(\mathrm{C}^+) = 9.5 \times 10^{-12} T_2^{-0.6}\ \mathrm{cm}^3\,\mathrm{s}^{-1} \tag{28}$$

(Tielens 2005;T05; Table 8.1). In our pedagogical model, $n_e = n(\mathrm{C}^+)$. Thus,

$$\frac{1 - x(\mathrm{C}^+)}{x(\mathrm{C}^+)^2} = n_b A_C \frac{\alpha_{rr}(\mathrm{C}^+)}{\zeta(\mathrm{C}^0)} \approx 3.6 \times 10^{-4} n_2 T_2^{-0.6} \tag{29}$$

where $n_2 = n_b/100\,\mathrm{cm}^{-3}$. Here, for the right term on RHS was evaluated with assuming $G_0 = 1$, $A_C = 10^{-4}$ and $\mathrm{A_V} = 0$. Clearly, most of the carbon will be ionized. Going forward, we assume that $x(\mathrm{C}^+) = 1$ but $1 - x(\mathrm{C}^+) \neq 0$. The volumetric heating rate is

$$\mathcal{H} = n_b \Gamma_{\mathrm{C}^0} \tag{30}$$

where

$$\Gamma_{\mathrm{C}^0} = \zeta(\mathrm{C}^0) A_C [1 - x(\mathrm{C}^+)] \langle E_{\mathrm{C}^0} \rangle \tag{31}$$

is the FUV photoionization heating rate, per H atom, by C^0. With the help of Equation 29, the above equation simplifies to

$$\mathcal{H} = n_b^2 A_C^2 x(\mathrm{C}^+)^2 \langle E_{\mathrm{C}^0} \rangle \alpha_{rr}(\mathrm{C}^+). \tag{32}$$

The principal cooling is via the fine structure line of C^+. If so, provided that the electron and H atom densities are below their critical densities (§2.1), the volumetric cooling rate is

$$\begin{aligned} \mathcal{L} &= [n_e n(\mathrm{C}^+) k_{01}(e) + n_{\mathrm{H}} n(\mathrm{C}^+) k_{01}(\mathrm{H})] E_{10} \\ &= n_b^2 [A_C^2 x(\mathrm{C}^+)^2 k_{01}(e) + A_C x(\mathrm{C}^+) k_{01}(\mathrm{H})] E_{10} \end{aligned} \tag{33}$$

where we approximated $n_{\mathrm{H}} = n_b$, given the small abundance of carbon relative to hydrogen. The values of E_{10}, $k_{10}(\mathrm{H})$ and $k_{10}(e)$ can be found in §2.1.

The temperature of the cloud can be derived by setting $\mathcal{H} = \mathcal{L}$. In the approximation we are using, $x(\mathrm{C}^+) = 1$. The classical simplification of Equation 33 retains electron collision (which has a T dependence similar as k_{10}) and ignores collisional excitation of C^+ by H (Sptizer 1978; [S78]; §6.2b) and results in

$$k_{01}(e, T) = \alpha_{rr}(\mathrm{C}^+) \frac{\langle E_{\mathrm{C}^0} \rangle}{E_{10}} \tag{34}$$

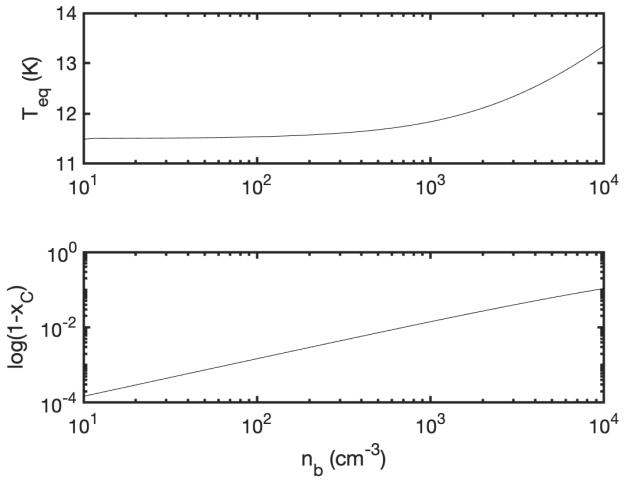

Figure 3: The run of equilibrium temperature (Top) and fraction of neutral carbon (Bottom) as a function of H atom density, assuming only heating via star light ionization of C I and radiative recombination.

– an equation which we could have constructed on physical grounds. For our choice of $\langle E_{\rm C^0}\rangle$, the resulting equilibrium temperature is 14 K and $1 - x({\rm C}^+) = 1.3 \times 10^{-5}$. Note that the inclusion of H collisions results in the reduction of the minimum temperature to 12 K. For densities which approach the critical densities, even within the pedagogical framework, we need to use the full framework described in §2.1, namely use $\mathcal{L}$ given by Equation 9. The run of temperature with density is shown in Figure 3. As expected the temperature rises once n_b and/or n_e exceeds critical densities. In this limit, the upper level population saturates to that given by the Boltzmann formula and so cooling is reduced with concomitant increase in temperature.

There are two additional concerns. First, we should evaluate the radiative excitation of the 158 μm line by the ambient field. Next, we should compute the optical depth of the C^+ line through the nebula. If the column density is sufficiently large then the cooling is reduced.

3.2 Photo-ionization of & Heating by Grains

Small grains including large molecules, particularly the Polycyclic Aromatic Hydrocarbons (PAHs; Tielens 2008; [T08]), play an out-sized role in the thermodynamics and chemistry of the diffuse interstellar medium (Watson 1972; [W72]). Numerically, for instance, the relative number of small PAHs to that hydrogen is 5×10^{-7} (REF; QUANTIFY). The principal reason for the major role of dust in the ISM is that dust grains and for that

matter PAHs have far more energy levels than that of atoms or ions. This opens up the entire FUV band for photoelectron heating. Equally, again in contrast to radiative recombination, dust grains, thanks to the availability of many energy states, can partake in charge exchange and recombination over a wide range of pre-collision and post-collision configurations.

As in a CCD, a photoelectron is liberated when an FUV photon is absorbed by a dust grain, typically at a depth of 100 Åwhich is larger than the typical mean free path for an electron in solid materials. The electron moves through the grain, heating the grain. In order to join the free electron pool the electron has to be energetic to overcome the work-function and the Coulomb field (if the grain was charged owing to prior photoelectron emission) of the grain. The work function of grains is smaller than that of bulk material (Watson 1972; [W72]).

In this model, the charge distribution of dust grains naturally depends on the radiation field, G_0. Grains will be increasingly charged positive as the strength of the radiation field increases. Equally, deeper into the cloud, where the FUV field is attenuated, grains will become increasingly neutral or even negatively charged up. The reader is referred to Tielens 2005; [T05] and Draine 2011 ([D11]) for a full elucidation of this rather complex subject.

Heating Rate. The typical work function for dust is 5 eV. The cross-section for photoelectric emission is zero at threshold and rises gradually. The primary radiation field that matters is in the range 8–13.6 eV. After accounting for the mean kinetic energy of electrons that recombine onto grains the net gain is about $\langle E \rangle \approx 1\,\mathrm{eV}$.

The photoelectric heating rate is dominated by small grains. Grains or PAHs with fewer than, say, 1000 carbon atoms contribute to half the heating rate and the remaining half is from grains with size of 15 Å to 100 Å. The total heating rate per unit volume is

$$n_b \Gamma_d = 10^{-24} \epsilon n_b G_0 \ \mathrm{erg\,cm^{-3}\,s^{-1}} \tag{35}$$

(Bakes & Tielens 1994; [bt94]) where the quantum efficiency is given by

$$\epsilon = \frac{4.87 \times 10^{-2}}{1 + 4 \times 10^{-3} \psi^{0.73}} + \frac{3.65 \times 10^{-2} T_4^{0.7}}{1 + 2 \times 10^{-4} \psi} \tag{36}$$

where $\psi = G_0 T^{1/2}/n_e$ which is proportional to the ratio of ionization rate to the recombination rate (Tielens 2005; [T05]; §3.3.3). For low value of ψ the heating rate is linearly proportional to the ambient FUV field, $\Gamma \approx 5 \times 10^{-26} G_0\,\mathrm{erg\,s^{-1}}$ per atom. However, for high value of ψ, the heating rate is independent of G_0 and is only related to $n_e n_b$.

In the CNM the peak quantum efficiency (≈ 0.05) can be realized. However, $\epsilon \approx 0.01$ in the WNM. The grain photoelectron heating can be compared with with photo-electron heating

by carbon, $\Gamma_{C^0} \approx 5 \times 10^{-26}[1 - x(C^+)]$ erg cm^{-3} s^{-1}. The heating rate from the latter is entirely decided by the ionization fraction of carbon which is close to unity. It is for this reason that photo-electron heating by dust dominates over that from C^0. Separately, at least in our neighborhood, it happens that the dust heating rate is larger than that due to cosmic rays (§3.3).

Ionization Equlibrium. Dust grains and PAHs may have strong affinity for electrons. That is wandering electrons may readily stick to grains and PAHs. The resulting PAH^- readily recombine with cations such as H^+ and C^+. In fact, these recombination coefficients are four to five orders of magnitude bigger than that of radiative recombinations. As a result, even after accounting for the small fraction of dust (relative to even C), "dust assisted" recombination can dominate the ionization fraction of elements (not just H but also ionizable metals such as C, Mg etc). Equally, charged grains, depending on their charge, can be neutralized by electrons or ions.

It is instructive to visit the pedagogical model that we discussed earlier, namely a nebula ionized, heated and cooled by only carbon. The grain-assisted volumetric recombination rate for a cation, X^+, is $n(X^+)n_b\alpha_{gr}(G_0, T, n_e)$ where the dependence on G_0 and n_e takes into account grain charging into account. Draine (2011; [D11]; Table 14.9) provides fitting formula for α_{gr} for various cations including H^+ and C^+. The ionization-recombination balance equation for carbon now has an additional path for recombination:

$$\zeta(C^0)[1 - x(C^+)] = n_e x(C^+)\alpha_{rr}(C^+) + n_b x(C^+)\alpha_{gr}(C^+) \tag{37}$$

which yields

$$x(C^+) = \frac{\zeta(C^0)}{\zeta(C^0) + n_e\alpha_{rr}(C^+) + n_b\alpha_{gr}(C^+)}. \tag{38}$$

Comparing Equation 28 to the above equation we can see that if the grain-assisted recombination term is larger than the radiative recombination then the carbon ionization fraction will be reduced.

While $\alpha_{rr}(C^+)$ depends only on T, $\alpha_{gr}(C^+)$ depends on n_e, G_0 and T. So the solution requires an iterative approach (Draine 2011; [D11]; §16.1.1). The resulting run of ionization as function of density is given in Figure 4. Clearly, grain-assisted recombination has a major impact on the ionization state of metals (and as we will see below on hydrogen as well). The reduction in the ionization of carbon translates to a higher photoelectric heating by C^0 (raising the gas temperature to 18 K at low density). To this we must add the considerable heating by dust itself. Thus CNM temperatures of 100 K can be explained.

Separately, it is worth noting that for, say, $\epsilon \approx 0.03$ and above $\langle E \rangle$ we find the grain ionization rate per atom is 3×10^{-14} s^{-1}. Thanks to large recombination coefficients the ionization rate, unlike that for C^0, is not limited by the availability of neutral species.

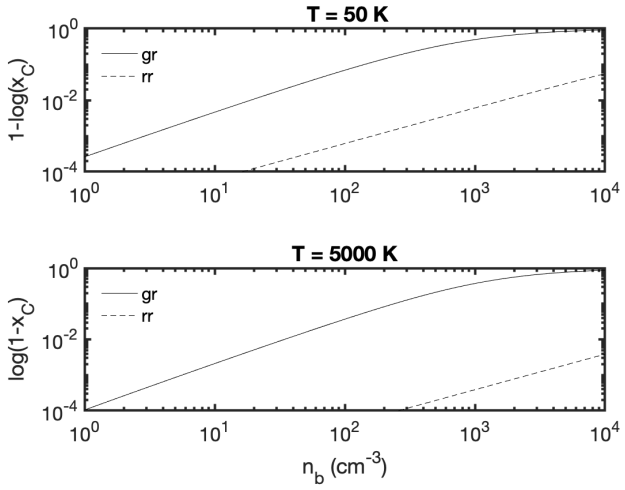

Figure 4: The run of carbon ionization as a function of particle density, n_b at two different temperatures. Carbon atoms are ionized by FUV and recombine via radiative recombination ("rr") or via a path involving grains ("gr"). Note the strong effect grain recombination has on the ionization fraction of the gas.

Recombination Cooling. We adopt the electron-grain recombination cooling from Bakes & Tielens 1(994; [bt94]):

$$\mathcal{L}_{\rm d,r} = 3.49 \times 10^{-30} T^{\alpha} \psi^{\beta} n_e n_H \ {\rm erg\,cm^{-3}\,s^{-1}} \tag{39}$$

where $\alpha = 0.944$, $\beta = 0.735 T^{-0.068}$

3.3 Ionization & Heating from Cosmic Rays

A cosmic ray moving faster than the Bohr velocity, αc where α is the fine structure constant, can ionize an electron in a hydrogen atom (and for that matter, helium also). The low energy cosmic rays, energy of a few MeV, naturally dominate this process. Unfortunately, the solar wind keeps such low energy protons from reaching Earth and so considerable extrapolation is needed in estimating the primary ionization rate (protons, helium). With this caveat the cosmic ray ionization rate is usually taken to be

$$\frac{dn_e}{dt} = 1.1 n_{\rm H} \zeta_{\rm CR} \Big(1 - \frac{x_e}{1.2}\Big) \Big[1 + \phi_s\Big] \tag{40}$$

where $\zeta_{\rm CR}$ is the primary ionization rate per H atom and

$$\phi_s = \Big(1 - \frac{x_e}{1.2}\Big) \frac{0.67}{1 + (x_e/0.05)} \tag{41}$$

is a multiplicative factor accounting for the secondary ionization (D11, §13.5). Each primary cosmic ray injects 35 eV of energy which goes into secondary ionization, heating and line excitation. The heating rate from cosmic rays from H/He ionization and Compton scattering of electrons is, respectively,

$$\Gamma_{\rm CR,}{}_n = 10^{-27} n_{\rm H} \Big[1 + 4.06 \Big(\frac{x_e}{x_e + 0.07}\Big)^{1/2}\Big] \Big(\frac{\zeta_{\rm CR}}{10^{-16}\,{\rm s}^{-1}}\Big) \ {\rm erg\,cm^{-3}\,s^{-1}}, \quad (42)$$

$$\Gamma_{\rm CR,}{}_e = 46 \times 10^{-27} n_e \Big(\frac{\zeta_{\rm CR}}{10^{-16}\,{\rm s}^{-1}}\Big) \ {\rm erg\,cm^{-3}\,s^{-1}} \quad (43)$$

(D11; §30.1).

4 Equilibrium Temperature & Ionization

In the previous three sections we discussed the injection of electrons and heat by photo-electron ionization of C^0, photo-electron ionization of dust and PAHs and ionization of H and He by cosmic rays. We are ready to construct the governing equations which determine the electron density, n_e and the temperature, T, of the cloud.

There are three sources of electrons: photo-ionization of metals with ionization potential less than that of hydrogen, photo-electron emission from dust grains including PAHs and ionization of hydrogen and helium by cosmic rays. The first contribution, dominated by carbon, is estimated to be about $x({\rm M}) \approx 1.5 \times 10^{-4}$. The number density of dust particles, relative to H, is extremely. Even if we consider PAHs (such as Pyrene, $C_{16}H_{10}$, through, say, Circumcoronene, $C_{54}H_{18}$, the relative number density is 5×10^{-7}. Thus, even if one assumes that all these particles are ionized, their contribution to the pool of electrons is small, $\sim 10^{-6}$. In fact, thanks to the large recombination coefficients, the PAHs are largely neutral (Tielens 2005; [T05]; §6.3.7). Thus while the photo-electron rate of dust and PAHs is high (§3.2) their contribution to the interstellar electron store is small when compared to that from C^0. We conclude that the main sources of electrons in diffuse medium is photo-ionization of C^0 and cosmic ray ionization of H and He. Additionally, cosmic rays, unlike FUV radiation, can penetrate dark clouds and so are, even with a low ionization rate, are important for dark clouds.

We will start off with the ionization-recombination equilibrium for photo-ionizable metals (M; cf. Equation 38):

$$x({\rm M}^+) = \frac{\zeta({\rm M}^0)}{\zeta({\rm M}^0) + n_e \alpha_{rr}({\rm M}^+, T) + n_b \alpha_{gr}({\rm M}^+, n_e, T, G_0)}. \quad (44)$$

We will simplify this by assuming that carbon represents all metals and thus set M=C in the above Equation and therefore set $A_C = A_M = 1.4 \times 10^{-4}$ (instead of the traditional

value of 1×10^{-4} for A_C). Next, we need an equation to determine the total electron denstiy, n_e. In order to compute the equilibrium n_e it is sufficient to consider the balance equation for a given species. For this purpose we will consider H I atoms. The atoms are ionized by cosmic rays. The resulting proton can recombine either via radiative recombination with an electron or with a dust/PAH particle. The resulting ionization-recombination balance equation is

$$\zeta_{\rm CR}(1+\phi_s)\Big[1-x({\rm H}^+)\Big] = n_b\alpha_{rr}({\rm H}^+)\Big[x({\rm H}^+)+A_M x({\rm M}^+)\Big]x({\rm H}^+)+n_b\alpha_{gr}({\rm H}^+)x({\rm H}^+). \quad (45)$$

The total electron ionization fraction is $x_e = x({\rm H}^+)+x({\rm M}^+)$. Finally we have the thermal balance:

$$n_b\Big[\Gamma_{{\rm CR},n}+x_e\Gamma_{{\rm CR},e}+\Gamma_d+\Gamma_{\rm C^0}\Big] = \mathcal{L}({\rm C}^+)+\mathcal{L}({\rm OI})+\mathcal{L}({\rm HI})+(g-f_r)n_b^2x_e^2\alpha_B k_B T \quad (46)$$

where we have assumed that cooling and heating is done at constant volume (isochoric), hence $g = 3/2$. In §2.4 we found that $f_r \approx 1$, through the entire range of temperature of interest.

These three coupled Equations 44–46 have to be solved numerically. The locus of the temperature, the proxy to the pressure, $\mathcal{P} = P/k_B$ and the metal and electron ionization fractions of a nebula in thermal and ionization equilibrium, subject to $G_0 = 1$ and $\zeta_{\rm CR} = 10^{-16}\,{\rm s}^{-1}$, is presented in Figure 5. The reflected "S" shaped locus is the signature result of the two-phase ISM model (Field, Goldsmith and Habing; 1969; [fgh69]). The inflection points marked A ($\mathcal{P} \approx 7200\,{\rm cm}^{-3}\,{\rm K}$, $T \approx 8,000\,{\rm K}$) and B ($\mathcal{P} \approx 1300\,{\rm cm}^{-3}\,{\rm K}$, $T \approx 300\,{\rm K}$) define the two branches, The lower branch, the cold neutral medium, is stable for $\mathcal{P} > 1300\,{\rm cm}^{-3}\,{\rm K}$ whereas the upper branch, the warm neutral medium, is stable for $\mathcal{P} < 7200\,{\rm cm}^{-3}\,{\rm K}$.

4.1 Comparison to previous work

The cooling and heating per atom of a nebula in ionization and thermal equilibrium is shown in Figure 6. The importance of dust heating is quite apparent. Notice the switch of cooling from the C^+ fine structure line to the OI fine structure line.

We have not included ionization and heating from soft X-rays. In some ways, cosmic ray heating can substitute for this lack of inclusion. The primary difference is that soft X-rays would preferentially ionize high-Z elements whereas cosmic ray predominantly ionizes hydrogen. The result is that an absorption spectrum of the nebula would be quite rich for X-ray ionization. Another issue that we have not considered is the optical depth to the C^+ line. This may become important for high density nebula with large column densities.

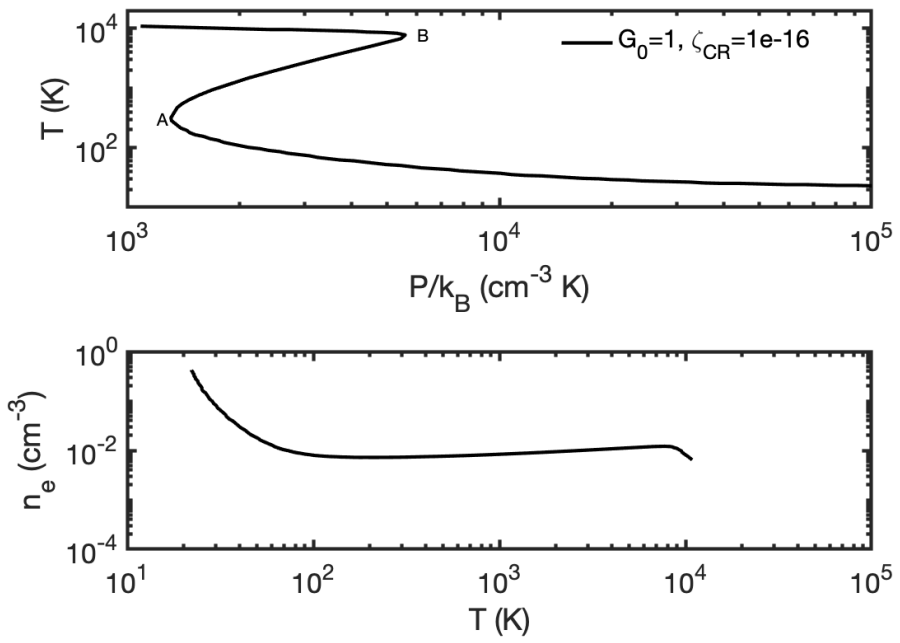

Figure 5: The locus of an optically thin interstellar nebula in thermal and ionization equilibrium. Top: Temperature versus the proxy to pressure, $\mathcal{P} = P/k_B$. Bottom: total ionization fraction ($x_H + x_M$) and metal ionization fraction (x_M).

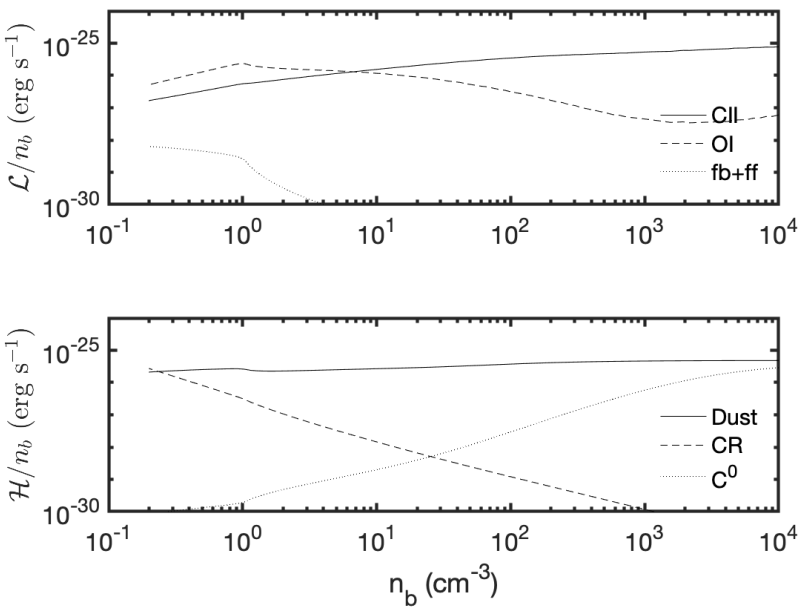

Figure 6: The cooling (top) and hearing (bottom) rate per atom of a nebula in ionization and thermal equilibrium for $G_0 = 1$ and $\zeta_{\rm CR} = 1 \times 10^{-16}\,{\rm s}^{-1}$.

5 A Nebula Irradiated by Strong Flux of Cosmic Rays

Our simple numerical modeling suite allows us to explore novel settings. For instance, explore the the equilibrium conditions for an H I cloud located in the general vicinity of a pulsar. Such clouds will experience a higher flux of cosmic rays. As can be seen from Figure 7 the inflection points are quite different from that of the fiducial case (for which the inflection points are marked by A and B). The points are now located as follows: $2200\,\mathrm{cm^{-3}\,K}$, 53 K and $10^5\,\mathrm{cm^{-3}\,K}$, 7900 K. The increased ionization in the CNM leads to stronger cooling and the result is that the maximum temperature on the CNM branch is 100 K. With increasing $\zeta_{\rm CR}$ the high pressure limit of the WNM branch is considerably extended. Despite higher cosmic ray rate the electron density remains low, either in the CNM or WNM.

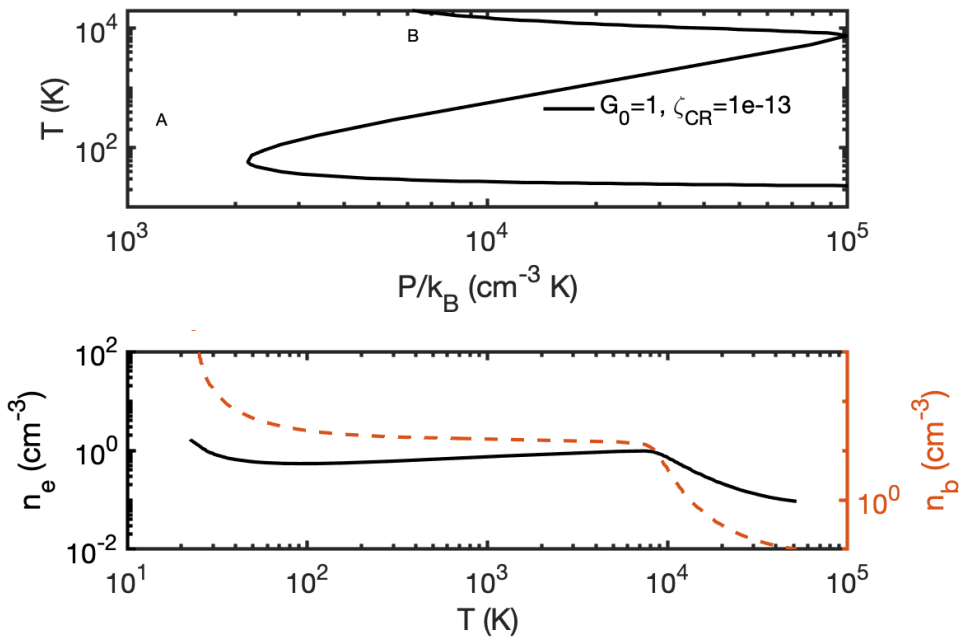

Figure 7: Same as Figure 5 but for $\zeta_{\rm CR} = 1 \times 10^{-13}\,\mathrm{s^{-1}}$.

The WNM branch should be regarded as illustrative and not accurate. We have ignored cooling via forbidden lines of OI, OII, NII and so on. Thanks to cooling via these forbidden lines the temperature will be below 10^4 K (and lower than that indicated in Figure 7). Next, cosmic rays will not only ionize H but also He, NI, OI and so on. Subject to variations in recombination coefficients the ionization fraction of He, NI and OI will follow that of

hydrogen. The nebula will be teeming with all sorts of ions, unusual for CNM such as N^+, Ne^+ and Ar^+ and will be a hotspot for gas-ion chemistry!